

Enhanced Cerebral but Not Peripheral Angiogenesis in the Goto-Kakizaki Model of Type 2 Diabetes Involves VEGF and Peroxynitrite Signaling

Roshini Prakash,^{1,2} Payaningal R. Somanath,^{1,2} Azza B. El-Remessy,^{1,2} Aisha Kelly-Cobbs,³ Javier E. Stern,³ Paula Dore-Duffy,⁴ Maribeth Johnson,⁵ Susan C. Fagan,^{1,2} and Adviye Ergul^{1,2,3}

We previously reported enhanced cerebrovascular remodeling and arteriogenesis in experimental type 2 diabetes. This study tested the hypotheses that 1) cerebral but not peripheral angiogenesis is increased in a spatial manner and 2) peroxynitrite orchestrates vascular endothelial growth factor (VEGF)-mediated brain angiogenesis in diabetes. Stereology of brain, eye, and skeletal muscle microvasculature was evaluated in control and diabetic rats using three-dimensional images. Migration and tube formation properties of brain microvascular endothelial cells (BMECs) were analyzed as markers of angiogenesis. Vascular density, volume, and surface area were progressively increased from rostral to caudal sections in both the cerebral cortex and striatum in diabetic rats. Unperfused new vessels were more prominent and the pericyte-to-endothelial cell ratio was decreased in diabetes. Vascularization was greater in the retina but lower in the peripheral circulation. VEGF and nitrotyrosine levels were higher in cerebral microvessels of diabetic animals. Migratory and tube formation properties were enhanced in BMECs from diabetic rats, which also expressed high levels of basal VEGF, nitrotyrosine, and membrane-type (MT1) matrix metalloproteinase (MMP). VEGF-neutralizing antibody and inhibitors of peroxynitrite, src kinase, or MMP blocked the migration. Diabetes increases and spatially regulates cerebral neovascularization. Increased VEGF-dependent angiogenic function in BMECs is mediated by peroxynitrite and involves c-src and MT1-MMP activation. *Diabetes* 61:1533–1542, 2012

Major complications spanning from coronary artery disease, peripheral arterial disease, and retinopathy to stroke contribute to the increased morbidity and mortality in diabetes. Increasing occurrence of diabetes in younger individuals is especially alarming when one considers the development of these complications over the course of the disease. Although impaired collateralization and angiogenesis play an important role in coronary artery disease and peripheral arterial disease, in diabetic retinopathy, excess angiogenesis leads to increased edema, bleeding, and ultimately resulting

in blindness (1–3). Our understanding of how diabetes affects cerebral vascularization is not equally clear.

Neovascularization can involve vasculogenesis, angiogenesis, and arteriogenesis (4–6). We reported extensive vascular remodeling and arteriogenesis in the pial vessels in Goto-Kakizaki (GK) rats, a lean and mild model of type 2 diabetes. We also showed that when an ischemic stroke is superimposed on this existing vascular condition, diabetic animals develop hemorrhagic transformation (i.e., bleeding into the infarct) and perform poorly on neurobehavioral tests (7). Prevention of pial remodeling by glycemic control or inhibition of matrix metalloproteinases (MMPs) was associated with reduced hemorrhagic transformation and improved neurologic outcome (8). The spatial and molecular regulation of angiogenesis and its impact on stroke outcome remain to be determined.

Reactive oxygen species (ROS) are involved in the regulation of neovascularization (9,10). Although low levels of ROS, peroxynitrite in particular, can propagate the angiogenic signal of VEGF, excess ROS can be detrimental and inhibit vascular endothelial growth factor (VEGF)-mediated cell survival (11–13). Inhibition of peroxynitrite prevents neovascularization in ischemic retinopathy (14). Building on these findings, we tested the hypotheses that 1) cerebral but not peripheral angiogenesis is increased in a spatial manner in the GK model of diabetes and 2) peroxynitrite orchestrates VEGF-mediated angiogenic signal in the brain microvasculature in diabetes.

RESEARCH DESIGN AND METHODS

Assessment of cerebral neovascularization. Weight-matched control and diabetic GK rats (male, 270–310 g) were used for the study in accordance with National Institutes of Health guidelines for the care and use of animals in research and under protocols approved by the Georgia Health Sciences University. Diabetic rats had higher blood glucose levels (95.3 ± 3.0 vs. 176.2 ± 7.5 mg/dL; $n = 19$). Animals were injected with 500 μ L of 50 mg/mL fluorescein isothiocyanate (FITC)-dextran (molecular weight 2,000,000; Sigma-Aldrich, St. Louis, MO) through the jugular vein under pentobarbital anesthesia. Brains were cut into 2-mm slices (labeled A–G rostral to caudal) (Fig. 1A) and processed in 4% paraformaldehyde (24 h) and 30% sucrose in PBS. Z-stacked confocal images of 100- μ m sections from regions B (anterior to the middle cerebral artery [MCA] comprising the frontal cortex-sensory, bregma 3 to 1), C (medial where the MCA branches out to supply the frontal motor cortex, bregma 1 to –1), and D (posterior to the MCA comprising of the parietal cortex, bregma –1 to –3) were acquired using Zeiss LSM 510 confocal microscope in the regions of interest (ROIs) within the cortex and striatum (Fig. 1B, indicated by yellow and orange squares). ROIs were based on our previous findings demonstrating the location of infarcts and hemorrhage in the diabetic and control rats (Fig. 1B). An overall representation of these regions was obtained by imaging ROIs from three different sections obtained from one slice. Values were obtained from each ROI, and a mean value of three images from each section was calculated. Each measurement from one animal comprised an average of nine images from either the cortical or striatal region. Retinal flat mount, gastrocnemius, and soleus muscles were prepared similarly in the same animals to assess neovascularization in different vascular beds. Z-step was defined as

From the ¹Charlie Norwood Veterans Administration Medical Center, University of Georgia College of Pharmacy, Athens, Georgia; the ²Program in Clinical and Experimental Therapeutics, University of Georgia College of Pharmacy, Athens, Georgia; the ³Department of Physiology, Georgia Health Sciences University, Augusta, Georgia; the ⁴Department of Neurology, Wayne State University School of Medicine, Detroit, Michigan; and the ⁵Department of Biostatistics, Georgia Health Sciences University, Augusta, Georgia.

Corresponding author: Adviye Ergul, ergul@georgiahealth.edu. Received 1 November 2011 and accepted 31 January 2012.

DOI: 10.2337/db11-1528

This article contains Supplementary Data online at <http://diabetes.diabetesjournals.org/lookup/suppl/doi:10.2337/db11-1528/-/DC1>.

© 2012 by the American Diabetes Association. Readers may use this article as long as the work is properly cited, the use is educational and not for profit, and the work is not altered. See <http://creativecommons.org/licenses/by-nc-nd/3.0/> for details.

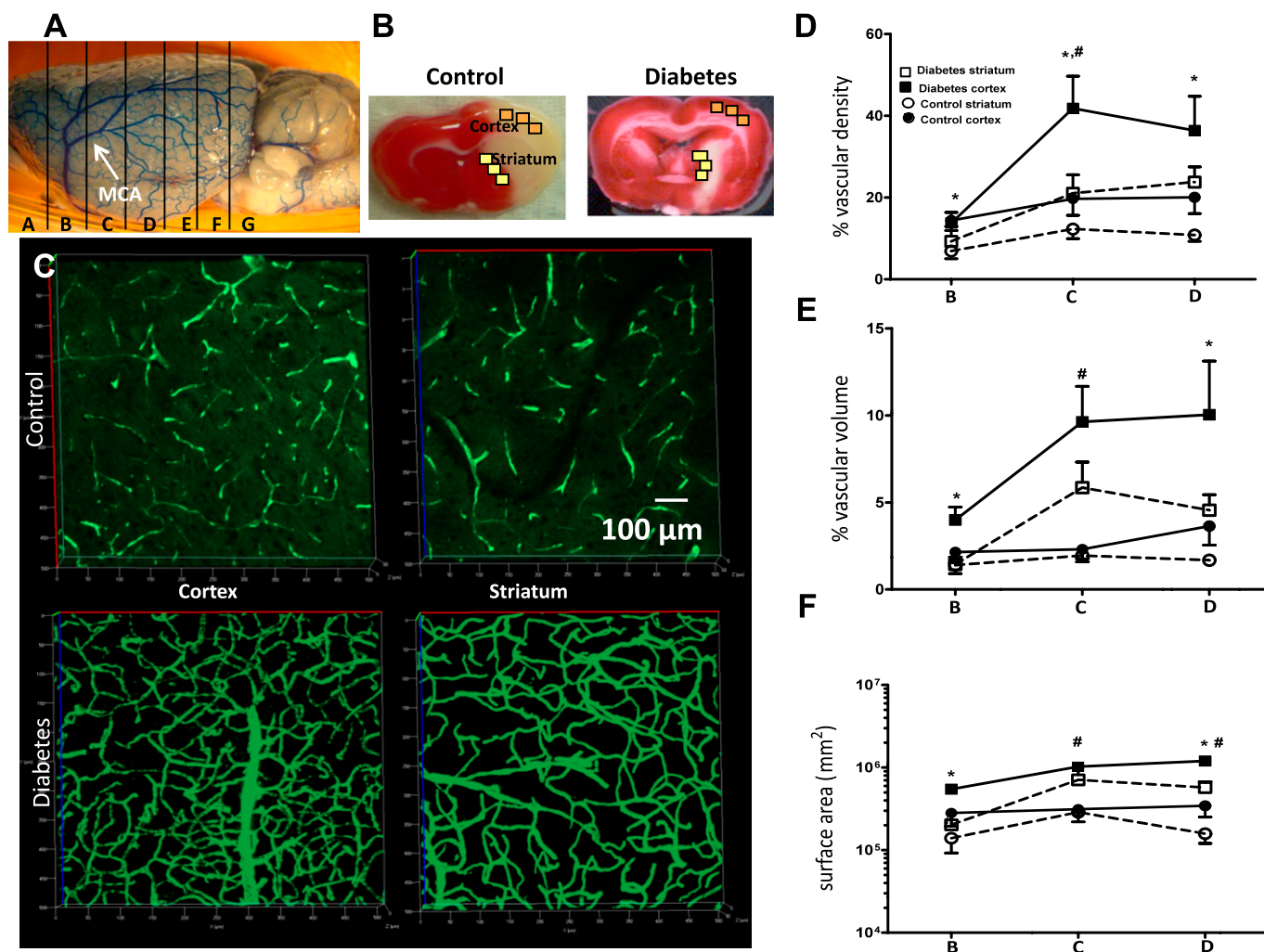


FIG. 1. Comparison of cerebral vascularization and its spatial distribution in control and diabetic GK rats. Different brain regions (A) and ROIs (B) where angiogenic parameters were assessed. C: Representative FITC-perfused cerebrovascular images from control and diabetic rats showing differences in angiogenesis in the cerebral cortex and striatum. D–F: Significant differences in vascular density (D), volume (E), and surface area (F) were observed between the cortex and striatum in both control and diabetic groups; however, diabetic rats exhibited a more than twofold increase in vascular density in the ROI in C and D. E and F: Vascular volume and surface area were markedly increased in both the cortex and striatum of the diabetic group compared with controls. * $P < 0.01$ cortex vs. striatum; # $P < 0.05$ diabetes vs. control. Data are means \pm SEM, $n = 4–11$. (A high-quality digital representation of this figure is available in the online issue.)

1.984 μm , image size 512×512 pixels, $25 \times$ lens. Image stacks were imported into Velocity (Improvision, Lexington, MA) and reconstructed three dimensionally. The FITC channel was classified to establish an intensity threshold, set to intensities five times above background immunofluorescence (calculated from random adjacent areas where no vasculature was observed).

Vascular density refers to the density of FITC-stained vasculature from the merged planes over the total area of the section. This parameter determines the change in vascularization in a given reference area and is independent of Z-function. Vascular volume refers to the ratio of the volume of the vasculature to the total volume (reference volume) of the section on a Z-stack (15). Surface area represents the absolute surface area of the vasculature, and a proportional increase in surface area with vascular volume represents increased vasculature.

To differentiate perfused and nonperfused immature vasculature, FITC-stained brain sections were costained with biotinylated isolectin B4 (Vector Laboratories, Burlingame, CA) overnight at 4°C . The sections were then incubated with Texas Red Avidin D (Vector Laboratories) for 2 h at room temperature. Images were acquired using a Zeiss confocal microscope, and colocalization measurements were carried out using Image J.

In vitro angiogenesis assays. Cell proliferation, migration, and tube formation assays were used as the indices of angiogenic potential of endothelial cells. Primary brain microvascular endothelial cells (BMECs) were isolated from control and GK rat brains by an immunomagnetic method of separation using Dynabeads. Whole brains were extracted under aseptic conditions, and the pial macrovasculature and the white matter was discarded. The cerebrum was minced and incubated overnight with collagenase/dispase (Roche,

Indianapolis, IN). Following incubation, the digestate was filtered through a $100\text{-}\mu\text{m}$ sieve and centrifuged, and the fraction containing microvascular segments were washed twice with PBS. Next, this fraction was incubated with CD31 antibody (BD Biosciences, Bedford, MA) for 4 h at 4°C and reincubated with secondary coated Dynabeads (Invitrogen, Carlsbad, CA) for 1 h. Cells attached to the Dynabeads were pulled down using a magnet; suspended in growth medium containing 10% FBS, 5% bovine calf supplement, 5 mmol/L glucose, and endothelial cell growth supplement; and cultured on fibronectin-coated flasks under standard 5/95% CO_2/air conditions. Cell proliferation assay was carried out by plating 70,000 cells, and the number of cells, cell volume, and diameters were measured using a Scepter automated cell counter (Millipore, Billerica, MA) 24 and 48 h after plating.

For the cell migration assay, cells were grown until confluency and serum starved for 8 h before performing the assay (16). A wound/scratch was created with a sterile pipette tip, and the distance uncovered was measured 24 h postscratch. During this time, no exogenous growth factors were added. An average of three measurements were taken, and the percentage recovery of scratch distance was calculated as $([\text{total scratch distance} - \text{average distance uncovered}]/\text{total scratch distance}) \times 100$. To determine the role of endogenous VEGF and downstream signaling in cerebral angiogenesis, the assay was repeated using cells pretreated with VEGF-neutralizing antibody (0.5 $\mu\text{g}/\text{mL}$; R&D Systems, Minneapolis, MN), peroxyinitrite decomposition catalyst 5,10,15,20-tetrakis(4-sulfonatophenyl) porphyrinato iron (III) chloride (FeTPPs) (2.5 $\mu\text{mol}/\text{L}$; EMD Biosciences, San Diego, CA), src kinase inhibitor PP2 (1 $\mu\text{mol}/\text{L}$; Calbiochem Cambridge, MA), and MMP inhibitor minocycline (100 $\mu\text{mol}/\text{L}$;

Sigma-Aldrich) for 2 or 24 h before the migration assay. In addition, control cells were cultured with conditioned medium collected from BMECs of diabetic rats with or without a VEGF-neutralizing antibody after the scratch was made.

For tube formation assay, 70,000 BMECs were suspended in reduced matrigel (BD Biosciences) mixed with serum free media and allowed to polymerize at 37°C. Tube-like structures were counted in a unit area at 24 and 48 h. **Assessment of pericytes.** For preparation of brain capillaries, tissue was homogenized as reported previously (17,18). The pellet was resuspended in 15% dextran in DMEM and passed through an 80- μ m nylon mesh. Microvessels were collected and resuspended in DMEM. Microvessels were >95% viable by trypan blue exclusion. In addition, exclusion of large vessels and the capillary nature of the preparation were confirmed by analysis on the Meridian ACAS 470 laser cytometer with computer-generated size determinations. Staining of microvessel preparations indicated that there were no neurons or glial-cell contaminants (17–19). Samples were allowed to adhere to coverslips and stained with 4',6-diamidino-2-phenylindole. To determine the number of pericytes, round nuclei were counted versus elongated nuclei (endothelial cells) (17,18). **Isolation of cerebral vessels.** Macro- and microvessels were isolated and homogenized in radioimmunoprecipitation assay buffer, as previously described (20). Homogenates were immunoblotted with VEGF and nitrotyrosine antibodies, as described below.

Immunoblotting. To measure the endogenous production of VEGF, BMEC supernatants were collected after serum starvation and incubated with 30 μ L of heparin agarose beads overnight at 4°C. After centrifugation, beads were boiled with loading buffer for 10 min, separated on 10% SDS gels, transferred to a polyvinylidene fluoride membrane, and incubated with anti-VEGF antibody (R&D Systems) overnight. Following incubation with secondary antibody, bands were visualized using ChemiGlow from Alpha Innotech (San Leandro, CA). All blots were stripped and reprobed with anti-actin antibody to ensure equal protein loading.

To study the effect of peroxynitrite formation on VEGF signaling, BMECs were pretreated with 2.5 μ M FeTPPS for 30 min and then challenged with 30 ng VEGF for 10 min. Published studies and our pilot findings (data not shown) showed that this protocol causes a rapid increase in peroxynitrite formation and VEGF receptor (VEGFR) phosphorylation (14). Cell lysates prepared in radioimmunoprecipitation assay buffer (35 μ g) were immunoblotted using antibodies against native and phosphorylated VEGF receptor 2 (VEGF-R2) (Cell Signaling Technology, Danvers, MA) anti-nitrotyrosine (Millipore, Billerica, MA), and native and phosphorylated c-src, MMP-2, and membrane-type (MT1)-MMP (Calbiochem). The proteolytic activity of MMP-2 in cell culture supernatants prepared from each group was determined by gelatin zymography (21).

Statistical analysis. Data are expressed as means \pm SE. Data were evaluated for normality, and appropriate transformations were used when necessary. Exact two-group Wilcoxon tests were used to study the effect of disease (control vs. diabetes). Exact tests are appropriate when a dataset is small, sparse, or skewed. A 2 \times 2 mixed-model repeated-measures ANOVA (RMANOVA) was used to study the effect of disease (control vs. diabetes) and area of the brain (cortex vs. striatum) and their interaction on log percent vascular density, vascular volume and surface area, and the ratio of percent nonperfused vasculature to total vasculature. A 2 \times 2 RMANOVA also was used to study the effect of disease and time (24 vs. 48 h) and their interaction on log number of tubes per loops and percent increase in proliferation. A one-way ANOVA was used to assess the effect of treatment for controls (none, diabetic endothelial cell-conditioned media (ECM), diabetic ECM + anti-VEGF antibody) on percent recovery of scratch distance in 24 h. A 2 \times 3 ANOVA was used to study the effect of disease and treatment and their interaction using VEGF-neutralizing antibody, FeTPPs, PP2, and minocycline as the treatments and measuring percent recovery at 24 h as the outcome. A Tukey test was used to adjust for the multiple comparisons for significant effects in the previous analyses. A one-way ANOVA within disease was used to study the effect of treatment (untreated, FeTPPs, VEGF, and FeTPPs + VEGF) on the ranked data for the phosphorylated VEGF-R2-to-VEGF-R2 ratio, nitrotyrosine, and the phosphorylated src-to-src ratio. A Dunnett test was used to compare treated with untreated groups for significant effects. Statistical significance was determined at $\alpha = 0.05$, and because of the small sample sizes for some of the variables a statistical trend was determined at $\alpha = 0.10$. SAS version 9.2 (SAS Institute, Cary, NC) was used for all analyses.

RESULTS

Diabetes-mediated cerebral angiogenesis is spatially regulated. In all sections (Fig. 1A and B, frontal sensory cortex [B], frontal motor cortex [C], and parietal cortex [D]), cortical vascular density, volume, and surface area were greater than in that observed in the striatum (Fig. 1D–F). Furthermore, diabetes significantly increased all these

parameters especially in the Fig. 1A, C area. There was a progressive increase (rostral to caudal) in both cortical and striatal vascular density, volume, and surface area in the diabetic group (Fig. 1D–F).

Diabetes uniquely mediates cerebral neovascularization while regressing the peripheral vasculature. Isolectin costaining of FITC-filled sections allowed differentiation of perfusing (FITC and isolectin colocalization) and nonperfusing (isolectin alone) vessels. In accordance with the Velocity data, the total vasculature was relatively greater in the diabetic group and more so in the cortex compared with controls. Greater colocalization of FITC and isolectin in the cortex and striatum of the control group (Fig. 2A and Supplementary Fig. 1A) indicated that vessels were more mature and more likely to be perfused. There was relatively more isolectin staining in diabetic sections, indicating that there are more newly formed and nonperfusing vessels in both the cortex and striatum in the diabetic group (Fig. 2B and Supplementary Fig. 1A). The ratio of pericyte to endothelial cell was significantly reduced in the diabetic group compared with the control group (Fig. 2B), providing additional evidence for the immature nature of the vessels in diabetes.

Neovascularization was compared in three different vascular beds. Although the vessels appeared remodeled and larger in diabetic animals, vascular density was significantly decreased in gastrocnemius muscles in the diabetic rats compared with controls (Fig. 2C and Supplementary Fig. 1B). There was a nonsignificant increase in vascular density in the diabetic retinal vasculature exhibiting collateralization (Fig. 2C and Supplementary Fig. 1B). Retinal capillaries also appeared kinked along the abluminal surface.

Angiogenic factors are increased in cerebral microvessels of diabetic animals. Because VEGF is the major angiogenic factor involved in diabetic retinopathy, VEGF protein levels were measured in micro- and macrovessel preparations. The VEGF dimer detected ~45 kDa was greater in the microvessels but not macrovessels of diabetic animals (Fig. 3A). Slot-blot analysis showed that these vessels also exhibit greater nitrotyrosine levels (Fig. 3B).

Cerebral microvascular endothelial cells exhibit increased angiogenesis. BMECs from diabetic animals showed tube-like structures within 1 day of incubation, whereas the control endothelial cells underwent tubulogenesis 2 days after incubation (Fig. 4A and B). Cell proliferation also was significantly increased in diabetes (Fig. 4C). BMECs from diabetic rats were morphologically different, as indicated by smaller diameter and volume (Fig. 4D and E).

Spontaneous cell migratory response was greater in diabetes (Fig. 5A and B). To study if a growth factor released by the diabetic endothelial cells had the ability to increase cell migratory response in control endothelial cells, the diabetic BMECs were serum starved and the ECM was collected after 24 h. Control BMECs grown in this conditioned media showed greater cell migration compared with control, and the presence of VEGF-neutralizing antibody restored the cell migratory properties to control levels (Fig. 5A–C). VEGF-A levels, especially the dimer form, were significantly increased in the culture media obtained from BMECs of diabetic rats (Fig. 5D and E).

Roles of peroxynitrite, c-src, and MMPs in endothelial cell migration. To demonstrate the involvement of VEGF and peroxynitrite signaling in the increased angiogenic response in diabetes, we first determined the basal levels of native and phosphorylated VEGF-R2, nitrotyrosine, native

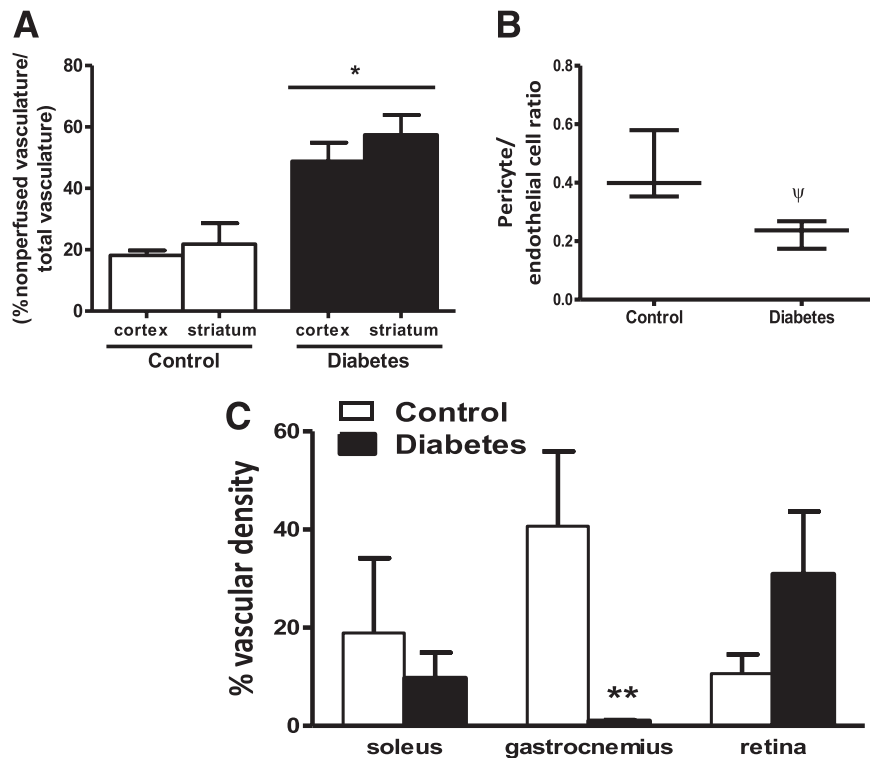


FIG. 2. Immature cerebral microvessels are more abundant in diabetes. **A:** Diabetic group had significantly increased cortical and striatal nonperfused vessels compared with controls. **B:** Pericyte-to-endothelial ratio was decreased in the diabetic group. **C:** There was a visual but not statistically significant increase in retinal vasculature, whereas peripheral vasculature was decreased in diabetes. * $P = 0.0016$ diabetes vs. control; $\psi P = 0.01$; ** $P = 0.029$ diabetes vs. control. Data are means \pm SEM, $n = 3-4$ (exact Wilcoxon test).

and phosphorylated c-src, as well as MT1-MMP and MMP-2. Phosphorylated VEGF-R2, phosphorylated c-src, and nitrotyrosine levels were greater in BMECs from diabetic animals compared with control cells (Fig. 6A–C). Although there was no difference in secreted MMP-2 (pro- or active form), cellular MMP-2 and MT1-MMP were higher in the diabetic BMECs compared with control (Fig. 6D–F).

To determine the roles of endogenous VEGF and downstream signaling molecules, including peroxynitrite, src kinase, and MMPs, in mediating the angiogenic response in BMECs, cells were pretreated for 2 or 24 h with either a VEGF-neutralizing antibody, FeTPPs, PP2, or minocycline, respectively, and cell migration at 24 h after treatment was assessed. With all treatments, there was a disease-and-treatment

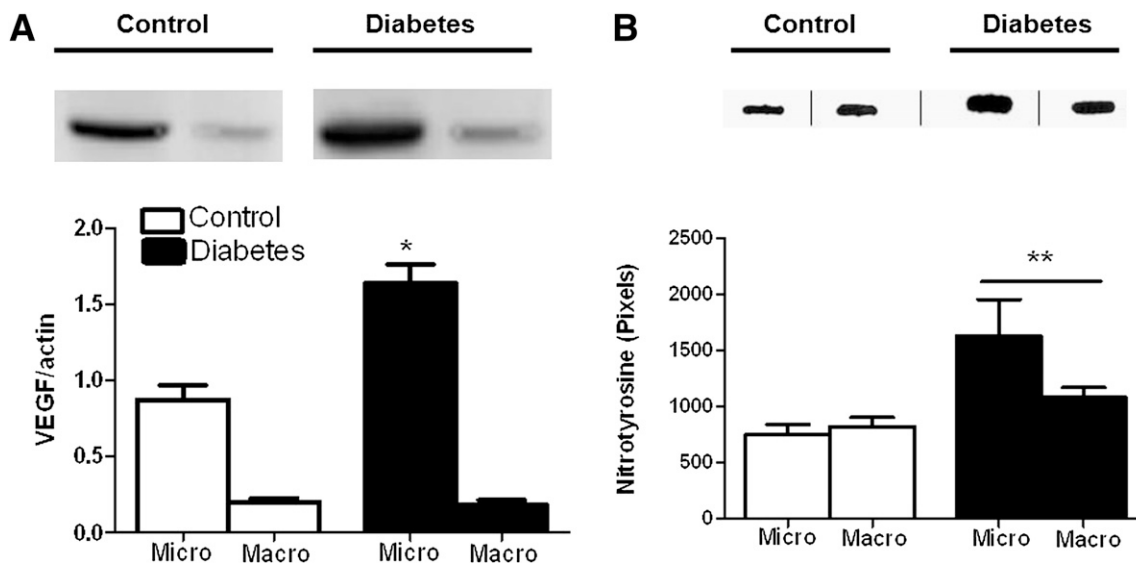


FIG. 3. Increased VEGF expression and tyrosine nitration status of micro- and macrovasculature in diabetes. **A:** VEGF levels were significantly increased in the cerebral microvasculature but not the macrovasculature in diabetes. **B:** Both diabetic micro- and macrovasculature had significantly increased tyrosine nitration compared with controls. * $P = 0.001$; ** $P = 0.05$ diabetes vs. control. Data are means \pm SEM, $n = 4$ (exact Wilcoxon test).

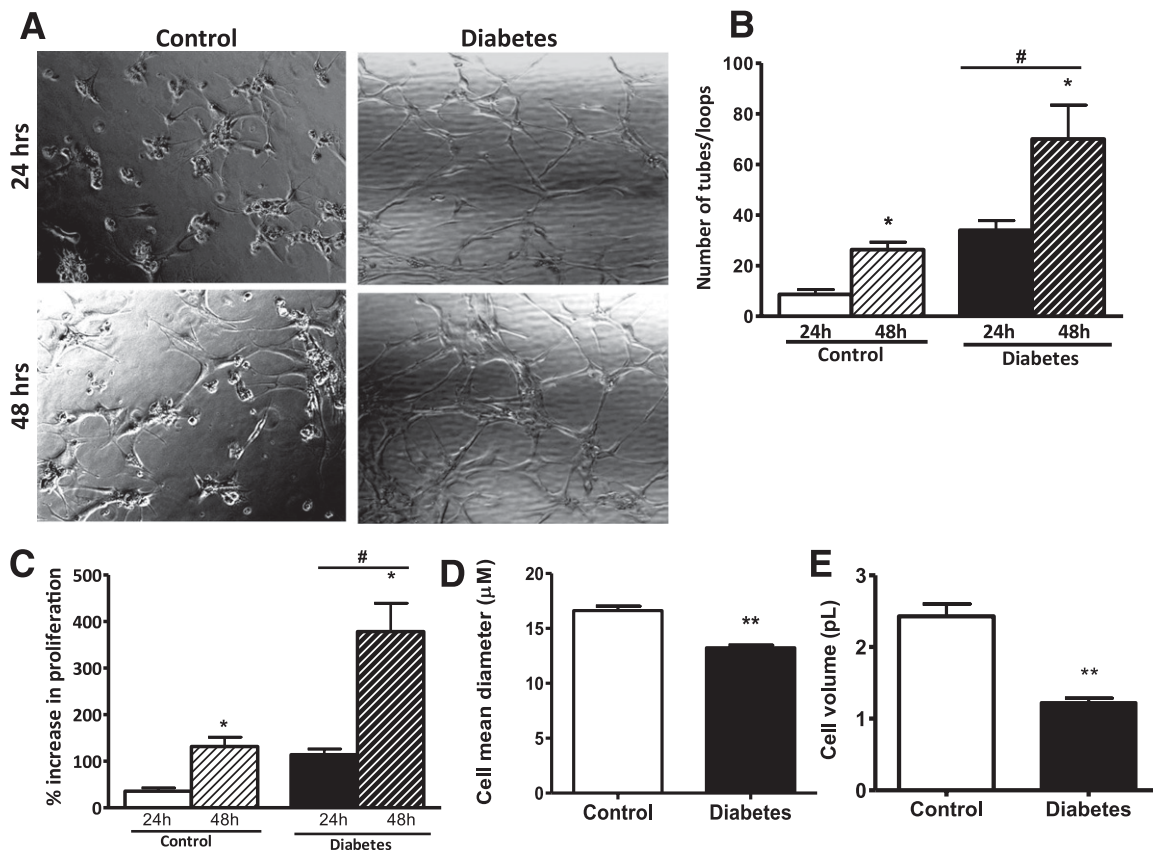


FIG. 4. Diabetic BMECs show significant increases in tubulogenesis over time. **A:** Representative images of BMECs showing more tube formation in the diabetic group after 24 and 48 h of plating on reduced matrigel. **B:** Diabetic BMECs have significantly increased tube formation properties after 24 and 48 h of plating on reduced matrigel than in control cells. **C:** Diabetic BMECs have a significantly higher percentage increase in proliferation after 24 and 48 h. **D** and **E:** Diabetic BMECs have significantly smaller cell mean diameter and volume compared with control cells, respectively. * $P < 0.01$ diabetes vs. control; # $P < 0.01$ 24 vs. 48 h; ** $P = 0.0022$ diabetes vs. control. Data are means \pm SEM, $n = 3-6$.

interaction such that treatments had no effect on the migratory response of control cells in the absence of an exogenous growth factor stimulation but reduced the migratory response of diabetic BMECs to levels seen in control cells (Fig. 7A–D).

Effect of peroxynitrite inhibition on VEGF signaling.

To determine how peroxynitrite modulates VEGF signaling, cells were first pretreated with FeTPPs and then stimulated with VEGF. The greater basal VEGFR and c-src activation as well as tyrosine nitration observed in diabetic cells were all reduced with FeTPPs (Fig. 8A–C), suggesting that peroxynitrite modulates VEGFR activation. Although VEGF stimulation increased VEGFR and c-src phosphorylation in control cells as expected, in diabetic cells there was no further increase. Pretreatment with FeTPPs prevented VEGF-stimulated VEGFR and c-src activation as well as protein tyrosine nitration in control cells. In diabetic cells, VEGF stimulation in the presence of FeTPPs yielded similar results to FeTPPs alone.

DISCUSSION

We have previously shown that cerebral neovascularization is stimulated in a mild model of type 2 diabetes, as evidenced by increased collateral number and diameter in the pial circulation (7,8,22). The goals of the current study were 1) to determine whether neovascularization also involves angiogenesis in this model; 2) if so, understand the spatial regulation and mechanism of this enhanced neovascularization;

and 3) investigate whether these vascular changes are unique to the cerebral circulation. The results provide intriguing new evidence that mild diabetes stimulates cerebral angiogenesis in a spatial manner, whereas it has an opposing effect on the peripheral vasculature. Furthermore, VEGF and peroxynitrite together are the key regulators of angiogenesis in cerebral microvascular endothelial cells via sequential activation of c-src followed by MMP-2 and MT1-MMP.

Diabetes is an exponentially expanding epidemic disease that leads to severe complications. Most diabetes complications have a significant vascular component and have been classified as either microvascular (nephropathy, retinopathy, and neuropathy) or macrovascular (heart disease, stroke, and peripheral arterial disease) (23,24). Macrovascular classification of stroke was mainly based on accelerated atherosclerosis in diabetes leading to narrowing of the carotid arteries. However, accumulating evidence suggests that small-vessel disease also is important for neurologic disorders such as dementia and stroke in patients with diabetes (25–27). These patients develop both large artery and terminal arteriole (lacunar) infarcts associated with increased incidences of bleeding (28–31). This line of clinical evidence emphasizes the need for preclinical studies focusing on the microvasculature of the brain in diabetes. Tissue-specific and spatial regulation of angiogenesis in experimental diabetes as we demonstrate in this study may be particularly significant for several reasons. First, we have reported that diabetic GK rats develop greater hemorrhagic transformation, especially around the infarcted

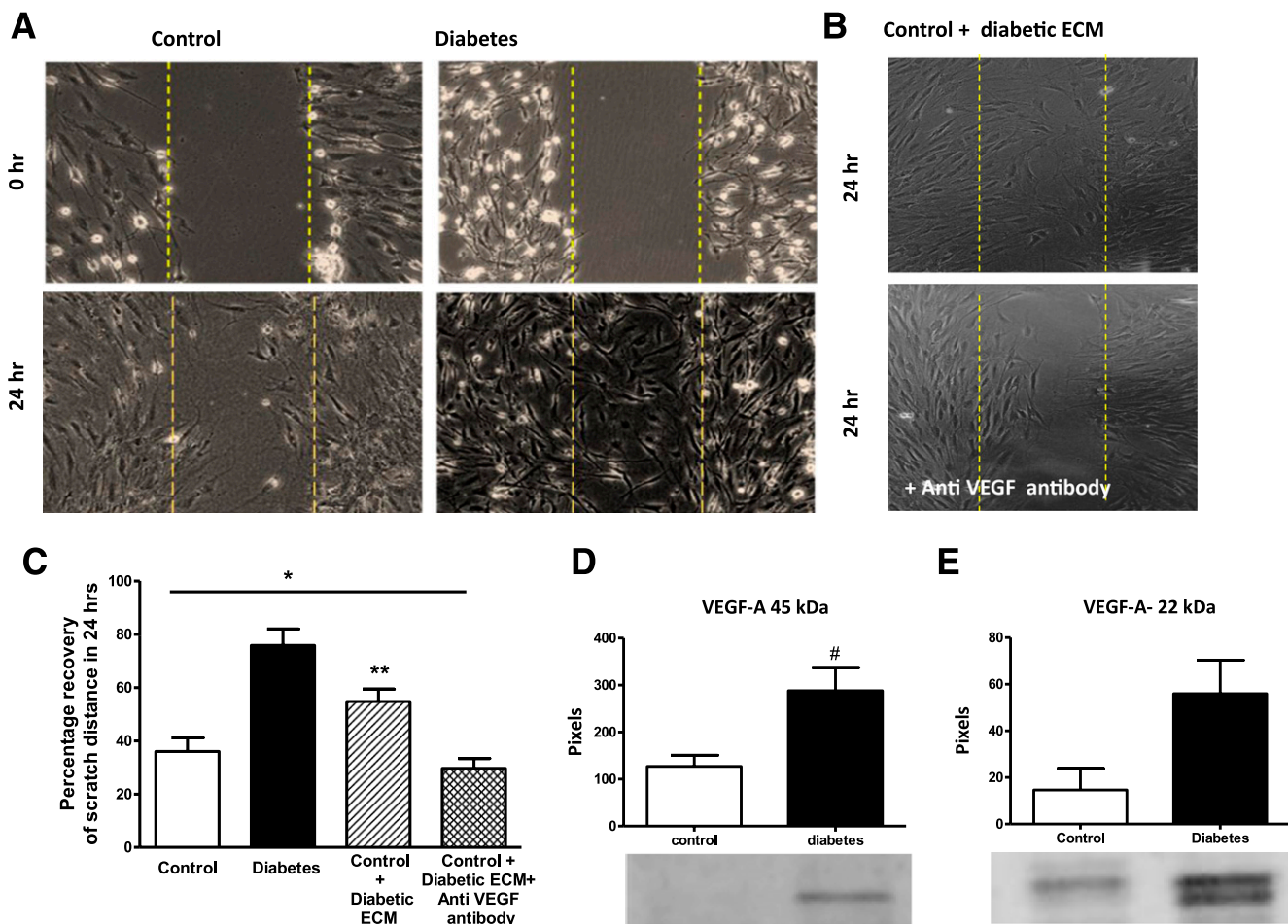


FIG. 5. Diabetic BMECs have increased cell migration that is mediated by VEGF in an autocrine manner. *A*: Representative images of BMECs showing increased spontaneous cell migration. *B*: Representative images of control cells treated with conditioned medium from diabetic cells in the presence and absence of VEGF-neutralizing antibody. Control BMECs treated with diabetic BMEC-conditioned media show increased cell migration and anti-VEGF antibody inhibits this effect significantly. *C*: Quantitative analysis of data shown in *A* and *B*. Diabetic BMECs plated on fibronectin show significantly increased spontaneous cell migration after 24 h. Control cells showed enhanced migratory properties when treated with diabetic endothelial cell-conditioned media (ECM), and VEGF-neutralizing antibody significantly abrogated this response. * $P = 0.0026$ across control groups; ** $P < 0.05$ vs. other control groups by Tukey post hoc analysis. Data are means \pm SEM, $n = 5-7$. *D* and *E*: Diabetic endothelial cells secrete relatively higher levels of native and dimerized VEGF-A. # $P = 0.016$ diabetes vs. control. Data are means \pm SEM, $n = 3-8$ (exact Wilcoxon test). (A high-quality color representation of this figure is available in the online issue.)

area upon temporary middle cerebral artery occlusion and have poor functional outcome (7,8). Differences in cerebrovascular architecture were previously observed within human cerebral cortex and between the striatum in rats and mice (32-34). Likewise, in this study we observed not only greater cerebral density of perfusing microvasculature in the cortex than in the white matter but also demonstrated that this difference is more pronounced in diabetic rats, which may partially explain smaller cortical infarcts in this model. Second, we now provide evidence that in addition to overall greater vascular density, there is more nonperfused new vessel formation in brain sections where we reported overt macroscopic bleeding in our past studies. Furthermore, there is less pericyte support indicative of the immature nature of these vessels, which may render the diabetic vessels more prone to reperfusion injury, leading to greater hemorrhagic transformation. Third, this pronounced neovascularization seems to be unique to the cerebral and retinal vasculature. As past studies reported, we also found impaired neovascularization of the skeletal muscle (35), whereas there was increased retinal vascular density and remodeling as seen in proliferative retinopathy

(36,37). Collectively, our results suggest that angiogenesis in the brain may explain the increased bleeding and vascular permeability that we reported in the diabetic animal model.

Endothelial cells are the first target of oxidative stress, matrix degradation, and metabolic changes occurring in diabetes. Micro- and macrovascular endothelial cells differ in function and protein expression at the organ level (38,39). Although past studies provided information on the molecular mechanisms of angiogenesis in retinal and coronary endothelial cells, little is known about cerebral microvascular endothelial cells (40-43). Furthermore, most if not all studies used either endothelial cell lines or primary cells isolated from normal animals to investigate the VEGF-mediated angiogenic response. The current study provide novel data by first studying brain microvascular endothelial cells and second by comparing the angiogenic potential of cells isolated from control versus diabetic rats. VEGF-A is a 22-kDa glycoprotein with five different isoforms, and it is one of the best-studied angiogenic factors (44). VEGF₁₆₅ is activated in diabetic retinopathy (14,45,46) and associated with retinal hematomas. Autophosphorylation of the VEGF-R2 upon VEGF binding and subsequent activation

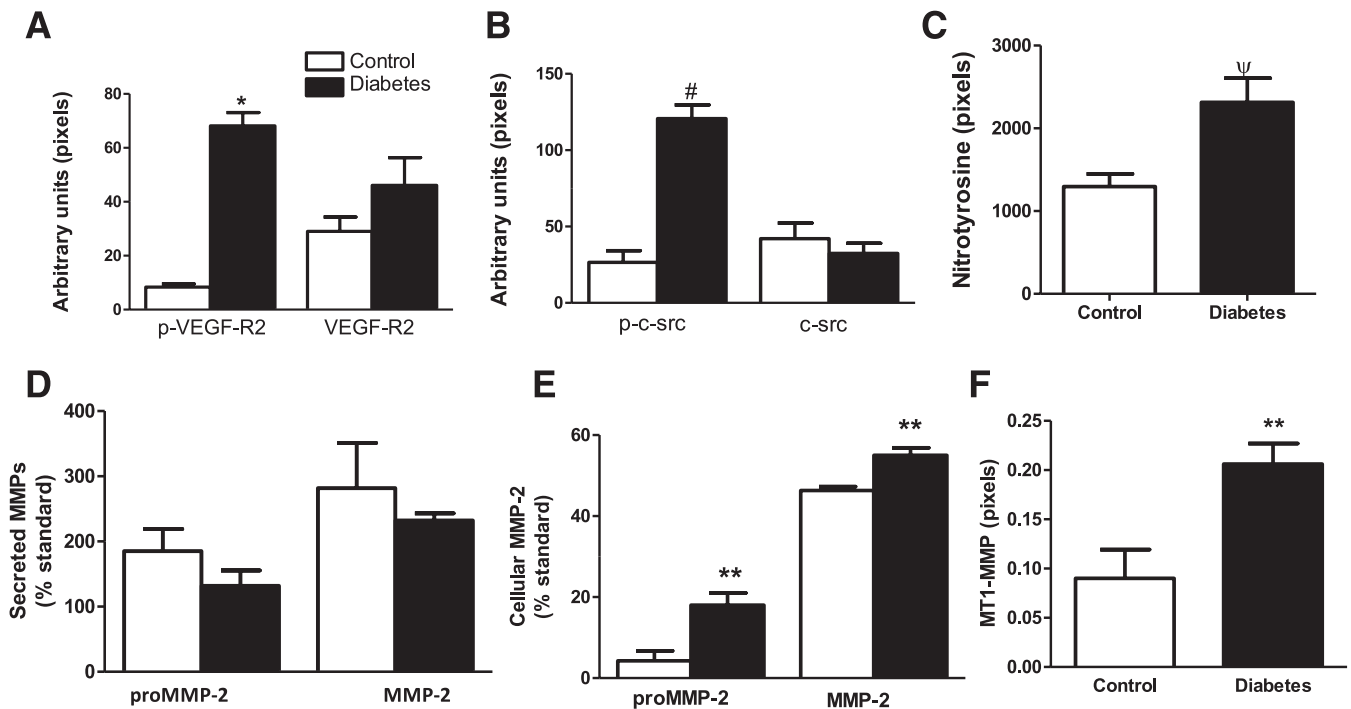


FIG. 6. Effect of diabetes on basal expression and phosphorylation status of angiogenesis mediators. **A:** Native and phosphorylated VEGF-R2 levels were determined by immunoblotting. Phospho-VEGF was increased in diabetic BMECs. Data are means \pm SEM, $n = 3$. **B:** In parallel with increased VEGF-R2 activation, c-src phosphorylation also was increased in diabetes. Data are means \pm SEM, $n = 4$. **C:** Diabetic endothelial cells have elevated protein tyrosine nitration compared with controls. Data are means \pm SEM, $n = 6-11$. **D and E:** MMP-2 activity was assessed by gelatin zymography. Although there was no difference in secreted latent and active MMP-2, cell-associated MMP-2 was significantly increased. **F:** MT1-MMP levels determined by immunoblotting were greater in diabetes. Data are means \pm SEM, $n = 3-4$. * $P = 0.0079$ diabetes vs. control; # $P = 0.029$ diabetes vs. control; $\psi P = 0.015$ diabetes vs. control; ** $P = 0.057$ diabetes vs. control (exact Wilcoxon test).

of c-src mediate the angiogenic effects. In our model, we found increased expression of soluble VEGF-A isoforms and its cognate receptor. Basal levels of the phosphorylated VEGF-R2 as well as c-src were higher, providing

evidence that the endogenous VEGF system contributes to enhanced angiogenic potential of brain microvascular endothelial cells in diabetes. Because these cells already are exposed to higher endogenous VEGF levels, further

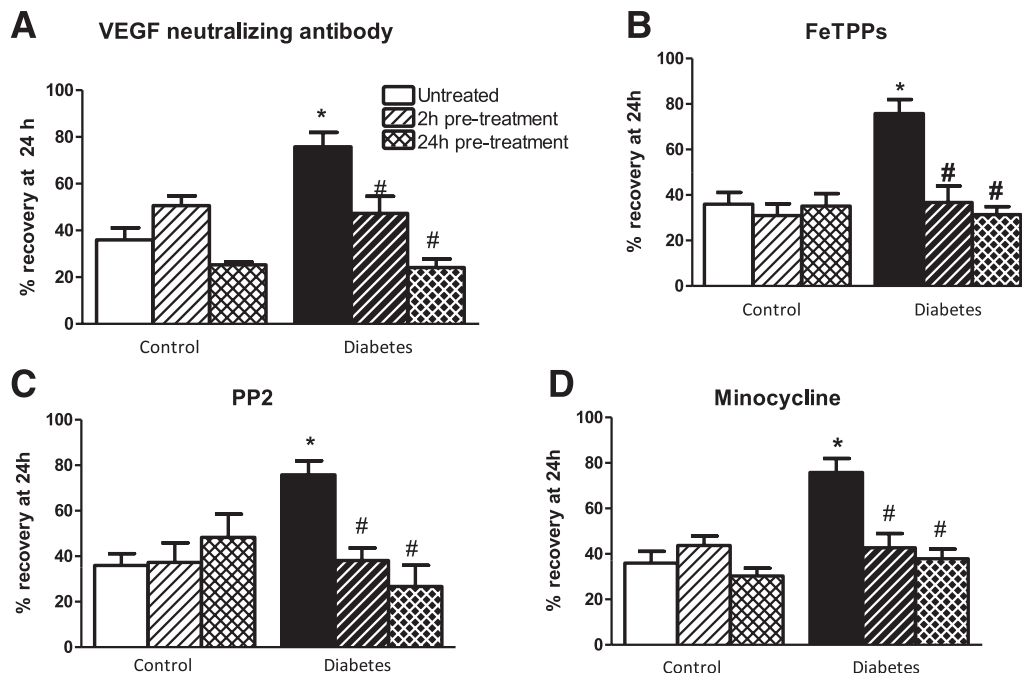


FIG. 7. Evidence for involvement of endogenous VEGF signaling in increased migration in diabetes. The role of various angiogenic proteins were assessed by using respective inhibitors on cell migration assays. Two- or 24-h pretreatment with anti-VEGF antibody (**A**), peroxynitrite decomposition catalyst FeTPPs (**B**), src inhibitor PP2 (**C**), or MMP inhibitor minocycline (**D**) significantly reduced migration of BMECs in diabetic but not control endothelial cells. # $P < 0.05$ vs. untreated diabetes; * $P < 0.01$ untreated diabetes vs. control. Data are means \pm SEM, $n = 4-7$.

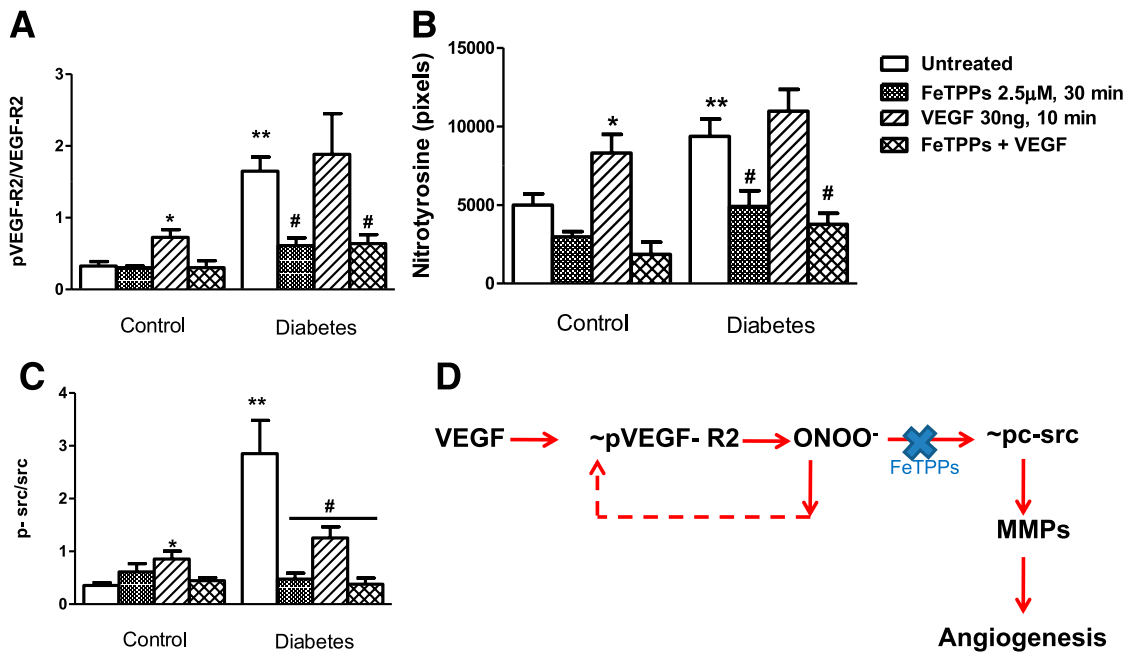


FIG. 8. The differential effect of exogenous VEGF on VEGF signaling in control and diabetic cells. Cells were treated with vehicle, peroxynitrite decomposition catalyst FeTPPs alone, VEGF alone, or VEGF plus FeTPPs. Phosphorylated VEGF receptor activation (p-VEGF-R2-to-VEGF-R2 ratio), peroxynitrite formation, and phosphorylated c-src activation (p-c-src-to-c-src ratio) were determined by immunoblotting, as shown in A–C, respectively. Exogenous VEGF treatment stimulated VEGF-R2 activation, c-src activation, and tyrosine nitration in control cells, and cotreatment with FeTPPs prevented this activation. Diabetic cells that show increased basal VEGF-R2, c-src, and nitrotyrosine activation do not show further elevation in response to exogenous VEGF but respond to FeTPPs treatment, indicating that peroxynitrite sustains VEGF-R2 phosphorylation and also mediates downstream signaling in these cells. **D:** Schematic representation of the role peroxynitrite in modulation of the angiogenic signal in brain microvascular endothelial cells. * $P < 0.05$ vs. other control groups; ** $P < 0.01$ vs. untreated control; # $P < 0.05$ vs. untreated diabetes. (A high-quality color representation of this figure is available in the online issue.)

stimulation with exogenous VEGF does not have an additional effect on VEGF-R2 activation that is seen in control cells, suggesting differential regulation of angiogenic signals in control and disease models.

Growing evidence suggest that reactive oxygen and nitrogen species such as peroxynitrite can act as signaling molecules and mediate VEGF's angiogenic properties (47). As depicted in Fig. 8C, we hypothesized that VEGF causes sequential stimulation of VEGF-R2, peroxynitrite, c-src, and MMPs and that peroxynitrite sustains VEGF-R2 phosphorylation, augmenting the angiogenic signal. Consistent with our hypothesis and our data with microvessel preparations and BMECs at baseline conditions, inhibition of VEGF, peroxynitrite, c-src, or MMPs completely prevented the greater migratory response in diabetic cells. When cells were stimulated with VEGF, control cells responded with increased VEGF and c-src phosphorylation, as reported in the literature with retinal microvascular endothelial cells, but diabetic cells did not show a further increase in VEGF or c-src activation, indicating that the system may be saturated. When cells were treated with FeTPPs, however, under baseline or VEGF stimulation conditions, VEGF-R2 phosphorylation was significantly decreased, confirming previous reports that peroxynitrite sustains VEGF-R2 activation and modulates the angiogenic signal in brain microvascular endothelial cells.

MMPs are involved in angiogenesis by degrading the matrix and allowing cells to migrate (48,49). MMP-2 and MT1-MMP, a secreted and membrane-bound form, respectively, are essential to initiate angiogenic responses. We have previously reported that increased MMP-2 and MMP-9 activities in brain micro- and macrovessels in our diabetes model (9,21). In the current study, we found

increased cellular MMP-2 activity and MT1-MMP protein. Moreover, treatment of cells with a broad spectrum MMP inhibitor minocycline prevented the cell migration in diabetes. We previously reported that chronic treatment of diabetic rats with minocycline prevents vascular remodeling and pial neovascularization in this model. Taken together, MMP activation contributes to angiogenic response of brain vascular endothelial cells. Of interest, we found that cellular, but not secreted, MMP-2 was increased in BMECs from diabetic animals, suggesting that either cells retain MMP-2 for another purpose or there is a defect in its secretion, which needs further investigation.

There are several limitations of the current study. First, we measured neovascularization and angiogenesis in a mild and lean model of diabetes, unlike the clinical conditions where diabetes and obesity are generally comorbid conditions. Blood glucose levels and resulting oxidative stress may be an important factor in the regulation of angiogenesis. However, this model helps us to tease out how moderate increases in blood glucose can contribute to pathological angiogenesis. As such, additional studies are needed to compare and contrast our findings with other models of diabetes. Second, we used an in vitro culture model to study the mechanisms of increased angiogenesis. However, cells isolated from diabetic rats retained their angiogenic potential and served as a good model. Third, we focused on VEGF, but involvement of other angiogenic factors cannot be ruled out. Nevertheless, there are novel and innovative aspects of this study that include 1) spatial characterization of angiogenesis in different brain regions that are relevant to neurovascular injury, 2) comparison of molecular signaling mechanisms that regulate emergence of capillaries under control and diabetic conditions, and

3) comparison of the angiogenic response in different vascular beds affected by diabetes. Collectively, our data advance our knowledge of cerebral angiogenesis in health and disease.

ACKNOWLEDGMENTS

This work was supported in part by VA Merit Awards (BX000891 to S.C.F. and BX000347 to A.E.), grants from the National Institutes of Health (NS063965 to S.C.F. and NS054688 to A.E.), and grants from the American Heart Association (EIA 0740002N to A.E. and 10PRE4030037 to R.P.).

No potential conflicts of interest relevant to this article were reported.

R.P. conducted the experiments and assisted with data analyses and manuscript preparation. P.R.S. assisted with isolation of brain microvascular endothelial cells. A.B.E.-R. provided assistance with the design of the studies involving VEGF and peroxynitrite inhibition. A.K.-C. assisted with animal studies and manuscript editing. J.E.S. provided assistance with the quantitative assessment of brain neovascularization using the Velocity program for analysis of confocal images. P.D.-D. provided assistance with pericyte studies. M.J. provided statistical analyses. S.C.F. was involved in data discussion and manuscript preparation. A.E. was in charge of the overall project from design to manuscript preparation. A.E. is the guarantor of this work and, as such, had full access to all the data in the study and takes responsibility for the integrity of the data and the accuracy of the data analysis.

Parts of this study were presented in abstract form at the American Stroke Association's International Stroke Conference 2012, New Orleans, Louisiana, 1–3 February 2012.

REFERENCES

- Aronson D. Hyperglycemia and the pathobiology of diabetic complications. *Adv Cardiol* 2008;45:1–16
- Brownlee M. The pathobiology of diabetic complications: a unifying mechanism. *Diabetes* 2005;54:1615–1625
- Celik T, Berdan ME, Iyisoy A, et al. Impaired coronary collateral vessel development in patients with proliferative diabetic retinopathy. *Clin Cardiol* 2005;28:384–388
- Carmeliet P. Mechanisms of angiogenesis and arteriogenesis. *Nat Med* 2000;6:389–395
- Heil M, Eitenmüller I, Schmitz-Rixen T, Schaper W. Arteriogenesis versus angiogenesis: similarities and differences. *J Cell Mol Med* 2006;10:45–55
- Peirce SM, Skalak TC. Microvascular remodeling: a complex continuum spanning angiogenesis to arteriogenesis. *Microcirculation* 2003;10:99–111
- Ergul A, Elgebaly MM, Middlemore ML, et al. Increased hemorrhagic transformation and altered infarct size and localization after experimental stroke in a rat model type 2 diabetes. *BMC Neurol* 2007;7:33
- Elgebaly MM, Prakash R, Li W, et al. Vascular protection in diabetic stroke: role of matrix metalloproteinase-dependent vascular remodeling. *J Cereb Blood Flow Metab* 2010;30:1928–1938
- Huang SS, Zheng RL. Biphasic regulation of angiogenesis by reactive oxygen species. *Pharmazie* 2006;61:223–229
- Nishikawa T, Araki E. Impact of mitochondrial ROS production in the pathogenesis of diabetes mellitus and its complications. *Antioxid Redox Signal* 2007;9:343–353
- el-Remessy AB, Bartoli M, Platt DH, Fulton D, Caldwell RB. Oxidative stress inactivates VEGF survival signaling in retinal endothelial cells via PI 3-kinase tyrosine nitration. *J Cell Sci* 2005;118:243–252
- Yun J, Rocic P, Pung YF, et al. Redox-dependent mechanisms in coronary collateral growth: the “redox window” hypothesis. *Antioxid Redox Signal* 2009;11:1961–1974
- Rocic P, Kolz C, Reed R, Potter B, Chilian WM. Optimal reactive oxygen species concentration and p38 MAP kinase are required for coronary collateral growth. *Am J Physiol Heart Circ Physiol* 2007;292:H2729–H2736
- El-Remessy AB, Al-Shabrawey M, Platt DH, et al. Peroxynitrite mediates VEGF's angiogenic signal and function via a nitration-independent mechanism in endothelial cells. *FASEB J* 2007;21:2528–2539
- Dockery P, Fraher J. The quantification of vascular beds: a stereological approach. *Exp Mol Pathol* 2007;82:110–120
- Liang CC, Park AY, Guan JL. In vitro scratch assay: a convenient and inexpensive method for analysis of cell migration in vitro. *Nat Protoc* 2007;2:329–333
- Dore-Duffy P. Isolation and characterization of cerebral microvascular pericytes. *Methods Mol Med* 2003;89:375–382
- Dore-Duffy P, Washington RA, Balabanov R. Cytokine-mediated activation of cultured CNS microvessels: a system for examining antigenic modulation of CNS endothelial cells, and evidence for long-term expression of the adhesion protein E-selectin. *J Cereb Blood Flow Metab* 1994;14:837–844
- Dore-Duffy P, Katychew A, Wang X, Van Buren E. CNS microvascular pericytes exhibit multipotential stem cell activity. *J Cereb Blood Flow Metab* 2006;26:613–624
- Harris AK, Hutchinson JR, Sachidanandam K, et al. Type 2 diabetes causes remodeling of cerebrovasculature via differential regulation of matrix metalloproteinases and collagen synthesis: role of endothelin-1. *Diabetes* 2005;54:2638–2644
- Portik-Dobos V, Anstadt MP, Hutchinson J, Bannan M, Ergul A. Evidence for a matrix metalloproteinase induction/activation system in arterial vasculature and decreased synthesis and activity in diabetes. *Diabetes* 2002;51:3063–3068
- Li W, Prakash R, Kelly-Cobbs AI, et al. Adaptive cerebral neovascularization in a model of type 2 diabetes: relevance to focal cerebral ischemia. *Diabetes* 2010;59:228–235
- Stettler C, Allemann S, Jüni P, et al. Glycemic control and macrovascular disease in types 1 and 2 diabetes mellitus: meta-analysis of randomized trials. *Am Heart J* 2006;152:27–38
- Akalin S, Berntorp K, Ceriello A, et al.; Global Task Force on Glycaemic Control. Intensive glucose therapy and clinical implications of recent data: a consensus statement from the Global Task Force on Glycaemic Control. *Int J Clin Pract* 2009;63:1421–1425
- Launer LJ. Diabetes: vascular or neurodegenerative: an epidemiologic perspective. *Stroke* 2009;40(Suppl.):S53–S55
- Saczynski JS, Jónsdóttir MK, Garcia ME, et al. Cognitive impairment: an increasingly important complication of type 2 diabetes: the age, gene/environment susceptibility: Reykjavik Study. *Am J Epidemiol* 2008;168:1132–1139
- Bourdel-Marchasson I, Lapre E, Laksir H, Puget E. Insulin resistance, diabetes and cognitive function: consequences for preventative strategies. *Diabetes Metab* 2010;36:173–181
- Castilla-Guerra L, Fernandez-Moreno MdelC. Stroke in diabetic patients: is it really a macrovascular complication? *Stroke* 2007;38:e106
- Idris I, Thomson GA, Sharma JC. Diabetes mellitus and stroke. *Int J Clin Pract* 2006;60:48–56
- Lüscher TF, Creager MA, Beckman JA, Cosentino F. Diabetes and vascular disease: pathophysiology, clinical consequences, and medical therapy: part II. *Circulation* 2003;108:1655–1661
- Mankovsky BN, Metzger BE, Molitch ME, Biller J. Cerebrovascular disorders in patients with diabetes mellitus. *J Diabetes Complications* 1996;10:228–242
- Cavaglia M, Dombrowski SM, Drazba J, Vasanji A, Bokesch PM, Janigro D. Regional variation in brain capillary density and vascular response to ischemia. *Brain Res* 2001;910:81–93
- Lauwers F, Cassot F, Lauwers-Cances V, Puwanarajah P, Duvernoy H. Morphometry of the human cerebral cortex microcirculation: general characteristics and space-related profiles. *Neuroimage* 2008;39:936–948
- Tsai PS, Kaufhold JP, Blinder P, et al. Correlations of neuronal and microvascular densities in murine cortex revealed by direct counting and colocalization of nuclei and vessels. *J Neurosci* 2009;29:14553–14570
- Suzuki E, Kashiwagi A, Nishio Y, et al. Increased arterial wall stiffness limits flow volume in the lower extremities in type 2 diabetic patients. *Diabetes Care* 2001;24:2107–2114
- Murata M, Ohta N, Fujisawa S, et al. Selective pericyte degeneration in the retinal capillaries of galactose-fed dogs results from apoptosis linked to aldose reductase-catalyzed galactitol accumulation. *J Diabetes Complications* 2002;16:363–370
- Ejaz S, Chekarova I, Ejaz A, Sohail A, Lim CW. Importance of pericytes and mechanisms of pericyte loss during diabetes retinopathy. *Diabetes Obes Metab* 2008;10:53–63

38. Ando H, Kubin T, Schaper W, Schaper J. Cardiac microvascular endothelial cells express alpha-smooth muscle actin and show low NOS III activity. *Am J Physiol* 1999;276:H1755–H1768
39. Garlanda C, Dejana E. Heterogeneity of endothelial cells. Specific markers. *Arterioscler Thromb Vasc Biol* 1997;17:1193–1202
40. Gordin D, Wadén J, Forsblom C, et al. Arterial stiffness and vascular complications in patients with type 1 diabetes: the Finnish Diabetic Nephropathy (FinnDiane) Study. *Ann Med* 3 November 2010 [Epub ahead of print]
41. Grauslund J, Green A, Kawasaki R, Hodgson L, Sjølie AK, Wong TY. Retinal vascular fractals and microvascular and macrovascular complications in type 1 diabetes. *Ophthalmology* 2010;117:1400–1405
42. Drel VR, Xu W, Zhang J, et al. Poly(ADP-ribose)polymerase inhibition counteracts cataract formation and early retinal changes in streptozotocin-diabetic rats. *Invest Ophthalmol Vis Sci* 2009;50:1778–1790
43. Whitmire W, Al-Gayyar MM, Abdelsaid M, Yousufzai BK, El-Remessy AB. Alteration of growth factors and neuronal death in diabetic retinopathy: what we have learned so far. *Mol Vis* 2011;17:300–308
44. Breen EC. VEGF in biological control. *J Cell Biochem* 2007;102:1358–1367
45. Caldwell RB, Bartoli M, Behzadian MA, et al. Vascular endothelial growth factor and diabetic retinopathy: role of oxidative stress. *Curr Drug Targets* 2005;6:511–524
46. Caldwell RB, Bartoli M, Behzadian MA, et al. Vascular endothelial growth factor and diabetic retinopathy: pathophysiological mechanisms and treatment perspectives. *Diabetes Metab Res Rev* 2003;19:442–455
47. Matsunaga T, Wartier DC, Weihrauch DW, Moniz M, Tessmer J, Chilian WM. Ischemia-induced coronary collateral growth is dependent on vascular endothelial growth factor and nitric oxide. *Circulation* 2000;102:3098–3103
48. Navaratna D, McGuire PG, Menicucci G, Das A. Proteolytic degradation of VE-cadherin alters the blood-retinal barrier in diabetes. *Diabetes* 2007;56:2380–2387
49. Giebel SJ, Menicucci G, McGuire PG, Das A. Matrix metalloproteinases in early diabetic retinopathy and their role in alteration of the blood-retinal barrier. *Lab Invest* 2005;85:597–607